chemosensors

Article

The Shell Structure Effect on the Vapor Selectivity of Monolayer-Protected Gold Nanoparticle Sensors

Rui-Xuan Huang [1], Chia-Jung Lu [2],* and Wei-Cheng Tian [3],*

[1] Department of Chemistry, Fu-Jen Catholic University, New Taipei 24205, Taiwan;
E-Mail: shanine401@gmail.com
[2] Department of Chemistry, National Taiwan Normal University, Taipei 11677, Taiwan
[3] Department of Electrical Engineering, National Taiwan University, Taipei 10617, Taiwan

* Authors to whom correspondence should be addressed; E-Mails: cjlu@ntnu.edu.tw (C.-J.L.);
wctian@cc.ee.ntu.edu.tw (W.-C.T.); Tel.:+886-2-7734-6132 (C.-J. L.); +886-2-3366-9852 (W.-C.T.).

Abstract: Four types of monolayer-protected gold nanoclusters (MPCs) were synthesized and characterized as active layers of vapor sensors. An interdigitated microelectrode (IDE) and quartz crystal microbalance (QCM) were used to measure the electrical resistance and mass loading changes of MPC films during vapor sorption. The vapor sensing selectivity was influenced by the ligand structure of the monolayer on the surface of gold nanoparticles. The responses of MPC-coated QCM were mainly determined according to the affinity between the vapors and surface ligands of MPCs. The responses to the resistance changes of the MPC films were due to the effectiveness of the swelling when vapor was absorbed. It was observed that resistive sensitivity to polar organics could be greatly enhanced when the MPC contained ligands that contain interior polar functional groups with exterior nonpolar groups. This finding reveals that reducing interparticle attraction by using non-polar exterior groups could increase effective swelling and therefore enhance the sensitivity of MPC-coated chemiresistors.

Keywords: gold nanoparticles; VOC sensors; chemiresistor; QCM

1. Introduction

The detection and control of volatile organic compounds (VOCs) remains a vital issue for air pollution in both industrial and residential areas. Because of their diversity of chemical functions and toxicity, rapid-response and highly selective sensors for VOCs are imperative for resolving the environmental problems associated with these compounds [1]. Commercially available VOC sensors are mostly based on metal oxide semiconductors that were developed many decades ago. Recently, there have been breakout developments in nanotechnology, and several novel nanomaterials have been applied to the innovative chemical sensors. These nanomaterials include carbon nanotubes, nano-TiO_2, and metal nanoparticles [2–4].

Monolayer-protected Au nanoclusters (MPCs) contain a nano-Au core with diameters of 2–6 nm and a self-assembled monolayer of organic thiolates on the nanoparticle surface. The highly stable Au-S chemical bond makes this material easy to preserve and use for a variety of applications without aggregations [5]. The organic shell allows this material to be suspended in various types of organic solvent and to be casted as a thin film. The semiconductor property and quantum dot effect of the nano-Au core can be readily studied. Various applications of this material, such as in catalytic reactions and electrode thin films, have been investigated [5,6].

One particularly interesting application is using MPCs as VOC sensors (*i.e.*, of volatile organic vapors) for environmental or biomedical detection [7–9]. The sensor response is based on the resistance changes that occur when organic vapors are absorbed. When a biased electrical field is applied to MPC film, the electrons can hop through Au nanoparticles and the current is measured. However, when electrons jump from one Au core to another, they must tunnel through an insulation region that was fabricated using two thiolate monolayers between the two Au-nanoparticles. When vapors are absorbed by the organic thiolates, the MPC film swells, and the distance between the Au cores increases. This phenomenon causes difficulty in electron tunneling and increases film resistance. As described in [6,7], the conductivity of an MPC film can be described as follows:

$$\sigma \propto e^{-2\delta\beta} e^{-E_c / kT} \tag{1}$$

where σ is the conductivity of the nanoparticle film, δ is the distance between two nanoconductive cores, β is the coupling constant, E_c is the activation energy, k is the Boltzmann constant, and T is the temperature in Kelvins. It is generally believed that an increase in δ plays a major role in MPC-coated chemiresistors. The dielectric constant of organic barriers, which is included in E_c, might contribute to resistive responses only when the absorbed vapor has a dielectric constant that differs substantially from that of the organic thiolates. For instance, the dielectric constants of regular VOCs such as aromatics, alkanes, or acetates are extremely close to that of the organic thiolates on the MPC surface. In cases detecting these compounds, the contribution of dielectric constant change is not crucial. Evan *et al.* demonstrated that water vapor or ethanol that has a considerably high dielectric constant could result in a reverse response in MPC-coated chemiresistors [10]. Recently, a new factor known as the "morphology effect" was explored by Haick's group [11,12]. This mechanism concerns mainly on the perforation or discontinuity of the MPC sensing film on the vapor responses. This perforation is mostly observed on ultra-thin film.

In the past decade, many researchers have contributed to this subject. Zellers *et al.* developed a single-phase synthetic approach that simplified the purification of this sensing material [13]. They sequentially developed several MPCs with diversified surface ligands and used these materials as detector arrays for µ-GC [14]. Zhong *et al.* used cross-linked MPC structures to stabilize the sensing film and obtain highly reliable performance [15]. Cai *et al.* and Konvalina *et al.* studied the effect of humidity on MPC-coated chemiresistors [16,17]. Steinecker *et al.* constructed a response model that incorporated both the partition coefficient and the free volume effect. The model could successfully predict the sensing behavior of the nonpolar octanethiol-capped MPC chemiresistors [18].

The first MPC material that was used for VOC sensors was octanethiol-capped MPCs [7]. This MPC material showed a better sensitivity to non-polar vapors rather than polar VOCs. The improved vapor recognition using branched alkane or aromatic groups has been demonstrated recently by Lewis and co-workers [19]. Our previous effort was focused on developing new MPC-sensing materials that have greater sensitivity to polar organic compounds [20]. We initially replaced octanethiol with highly polar ligands such as 2-naphthalenethiol, 2-benzothiazolethiol, and 4-methoxythiolphenol. Although we successfully increased the absorption mass of polar organic vapor on MPC films (*i.e.*, by conducting quartz crystal microbalance experiments), the responses on a chemiresistor platform was consistently less sensitive than that on octanethiol-capped MPCs. This previous finding triggered the hypothesis of the present study. We believe it is the strong attraction between the polar groups of surface thiolates that inhibits the swelling between nanoparticles. Therefore, in this study, we attempted to synthesize MPCs with a surface structure that had polar groups inside to attract polar gas molecules; and non-polar (alkane) groups outside as a divider between nanoparticles, which could reduce the interparticle attraction. The comparison of different selectivity between the chemiresistor and the QCM array was used to reveal the mechanism of the sensing behavior. The goal of this study was to develop MPC alternatives for octanethiol MPCs that provide different selectivity and a higher sensitivity to polar VOCs.

2. Experimental Section

2.1. Nanoparticle Material Synthesis

MPCs were synthesized using a two-phase approach [5]. The four surface monolayers of thiolates selected for capping Au nanoparticles were n-octanethiol (Au-C8), isooctyl 3-mercapropionate (Au-EST), a mixture of n-octanethiol and 3-mercaptopropionic acid (MixCOOH), and a mixture of n-octanethiol and 4-pyridinethiol (MixPT). The chemical structures of the four MPCs are shown in Figure 1. The synthetic approach for preparing the two pure ligand MPCs, Au-C8 and Au-EST, was as follows: 0.10 g of $HAuCl_4$ was dissolved in 8 mL of deionized water; 0.16 g of tetraoctylammonium bromide (TOAB) and 17 µL of n-octanethiol or isooctyl 3-mercapropionate were dissolved in 40 mL of toluene. The aqueous $HAuCl_4$ solution was added to the TOAB/toluene solution and stirred. The reducing agent, prepared by dissolving 0.112 g of $NaBH_4$ in 8 mL of water, was added to the stirred toluene/water solution. A rapid color change from yellow to deep purple was immediately observed. Vigorous stirring was continued for 1 h at room temperature. MPCs with mixed thiolate shells (*i.e.*, MixCOOH and MixPT) were synthesized using a ligand place-exchange reaction of n-octanethiol

with 3-mercaptopropionic acid or 4-pyridinethiol. A 0.2 μL aliquot of 3-mercaptopropionic acid or 4-pyridinethiol was added to the Au-C8/toluene solution and the resulting solution was stirred for 3 h. During this step, only a portion of the octanethiol could be replaced by either 3-mercaptopropionic acid or 4-pyridinethiol. Purification was achieved by reprecipitating the MPCs in a large quantity of cold ethanol to remove the excess TOAB or thiolates. The final products were redissolved in dichloromethane and dried for future use.

Figure 1. Chemical structures of four monolayer protected gold nanoclusters.
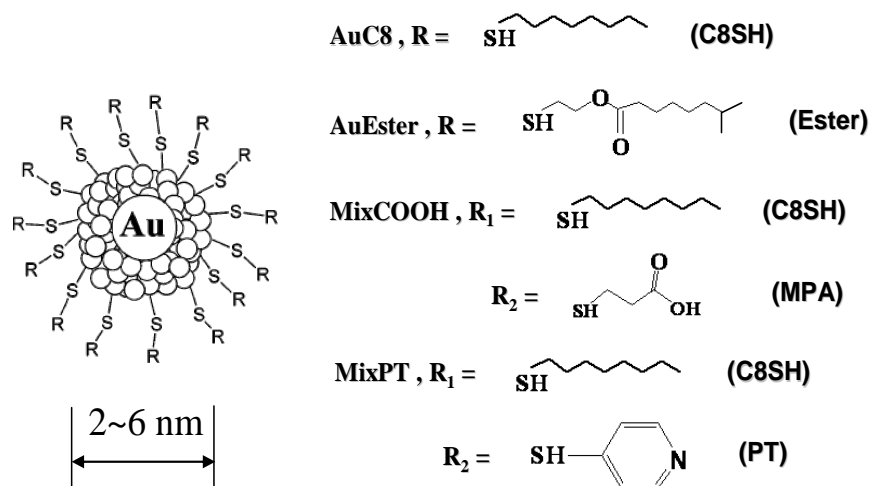
2.2. Quartz Crystal Microbalance and Chemiresistor Devices

The photos of both sensor devices are shown in Figure 2. The 10 MHz Au-surfaced electrode quartz crystals were purchased from Taitein Electronics Co., Taiwan. The driving circuitry was constructed in-house. The frequency output was measured using a counter/timer card (PXI-6522, National Instruments, TX, USA). Interdigit Au electrodes (IDE) for chemiresistor measurements were fabricated on a Si wafer, using standard photolithography and liftoff processes. Two pairs of interdigit electrodes were used for each MPC chemiresistor unit. We only measured one pair of the electrodes; the additional pair of electrodes was a spare in case the first failed during fabrication or coating. Each electrode had 40 pairs of interdigit fingers, with a 15 μm line width, 10 μm spacing, and 1.5 mm length. The active area of each sensor was 3 mm^2. Both devices were thoroughly cleaned using deionized water and ethanol and dried at 100 ℃ prior to coating. An MPC solution was prepared by redissolving MPCs in dichloromethane, and the solution was sprayed on the surface of the quartz crystal microbalance (QCM) and IDE. The side view of the MPC coated IDE was shown in Figure 2c. The sensing film was smooth and continuous. Therefore, the mechanism for perforation or discontinuous film does not apply to our study.

Figure 2. Photos of (**a**) quartz crystal microbalance (QCM) (**b**) interdigitated microelectrode (IDE) sensor devices and (**c**) SEM image of monolayer-protected gold nanocluster (MPC) coated IDE.
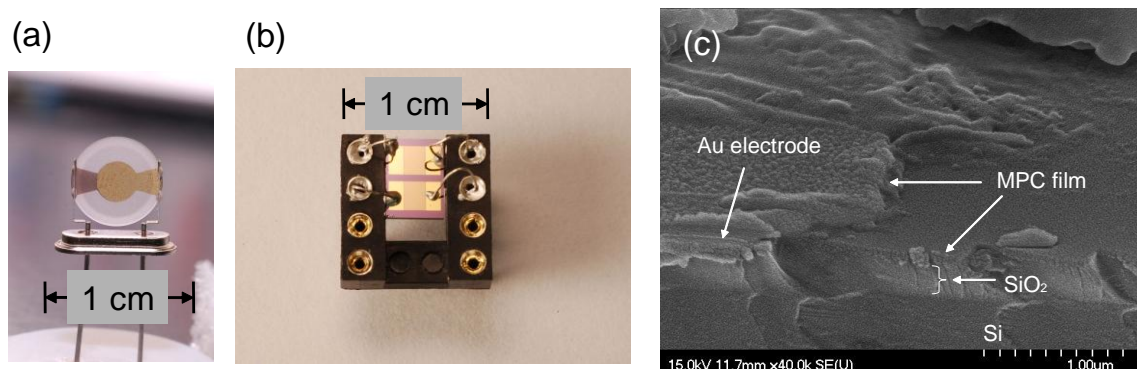
2.3. Vapor Generation System

Test organic vapor concentrations were generated using a dynamic system comprising three mass flow controllers, stainless steel or Teflon manifolds, adsorbent traps, and a solvent evaporator. Clean background air was obtained by passing compressed house air through consecutive layers of molecular sieve, charcoal, and particle filter to remove moisture, VOCs, and fine particles, respectively. The temperature was in equilibrium with the air conditioned lab, which was within 25 ± 1 °C. The humidity of the gas stream was kept below 2% RH at all time in order to observe the interaction between the sensing film and vapors without the interference of the moisture. The background air was passed through a bubbler to produce a saturated vapor concentration and was diluted to the desired concentration with various ratios of background air controlled by mass flow controllers (5850i, Brooks Instrument, PA, USA). Two solenoid three-way valves were connected in front of the test cell and vent that allowed computer-controlled switching between the background air and test vapor flow. The cleanness of the background air and the generated vapor concentration was confirmed using GC-FID (HP5890, Agilent). The test cell for housing both sensors had an internal volume of approximately 250 mL. The volumetric flow rate was >5 L/min to ensure the rapid switching between test concentration and background air.

3. Results and Discussion

3.1. Response Signals of MPC-Coated Sensors

Figure 3 provides examples of the response signals of four MPCs coated on IDE and QCM *versus* 1,000 ppm and 2,500 ppm toluene. The signals of the chemiresistor were measured using bridge circuitry and high input impedance operational amplifiers. The changes of resistance were converted to voltage. The increase in voltage was proportional to the increase in film resistance. As seen in Figure 3a–d, all the sensors responded rapidly when vapor was introduced. The resistance reaches a plateau as the vapor sorption reaches equilibrium. The signal heights of the three replicates are reproducible, and all sensors could return to their baseline when clean air was switched in. In Figure 3e–h, the vapor sorption by the MPCs caused a mass increase on the surface of the QCM and

caused a negative shift in frequency. The resolution of our QCM frequency counter was 1 Hz. The range of response signal was 10–40 Hz, depending on the materials and tested vapor. Therefore, some stair-like signal changes were observed because of the limits of the counter resolution. In addition, minor baseline drift was found, as shown in Figure 3f,h. In general, the MPC chemiresistor sensor had a better signal-to-noise ratio than did the QCM coated with the same MPCs.

Figure 3. Original response signals of four MPCs sensing materials coated on IDE (**a**–**d**) and QCM (**e**–**h**). Test condition: three replicates of 1,000 ppm and 2,500 ppm toluene.
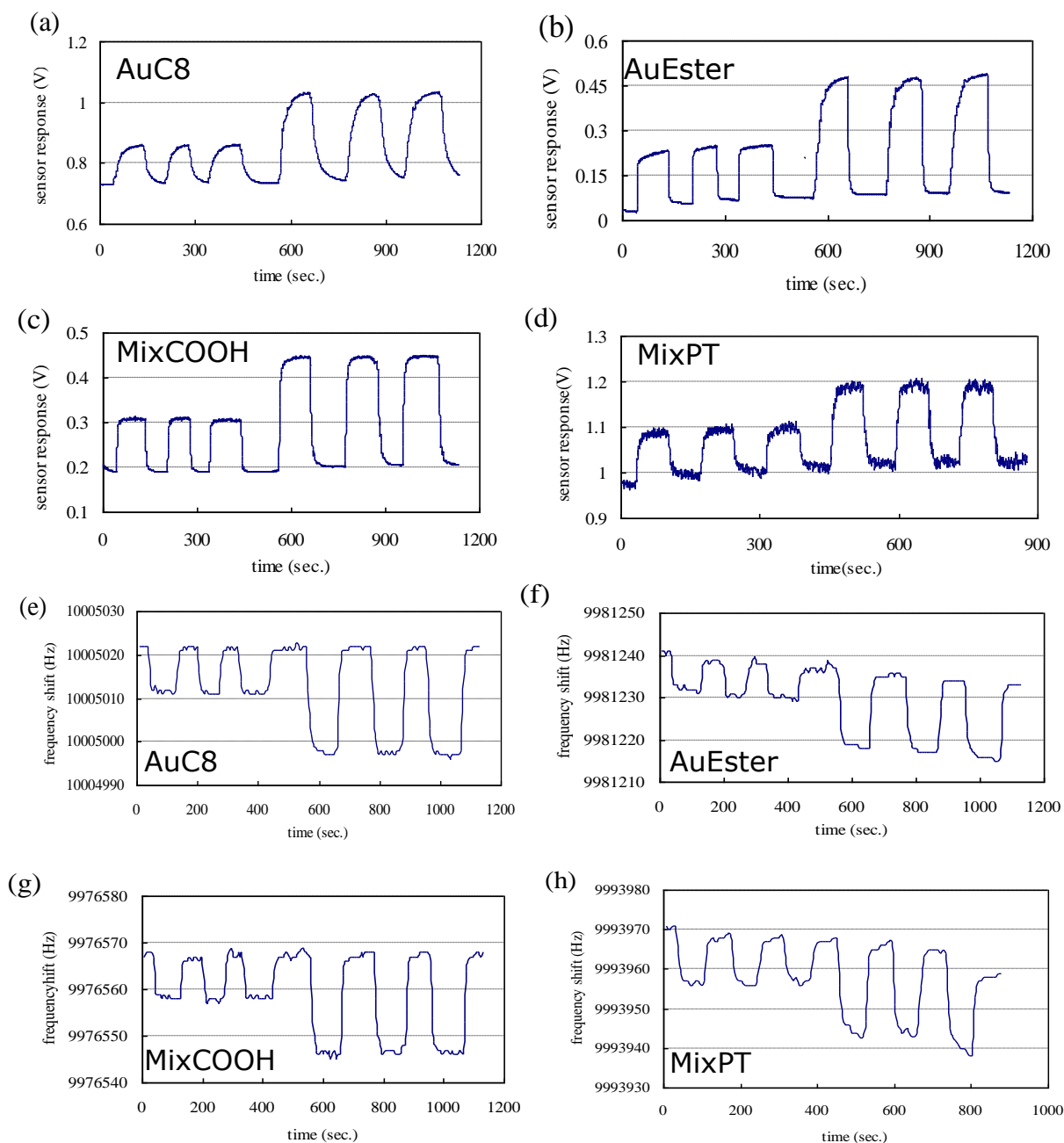

3.2. Calibration Curves of MPC-Coated Sensors

Figure 4 shows examples of the calibration curves of two compounds, octane and butyl acetate, tested with four MPCs on both QCMs and chemiresistors. The Y-axis units for the QCM array were

$\Delta f/f_0$, which stands for the vapor response frequency shift (Δf) normalized to film coating frequency shift (f_0). The primary output signal of the chemiresistor array was voltage, and we converted it into the change in resistance (ΔR) by using Ohm's law. The Y-axis units for the chemiresistor array calibration were expressed as $\Delta R/R$, which represents the change in resistance normalized to their baseline resistance in clean air. The units on the Y-axes of Figure 4 are in ppm for frequency or resistance changes. The slopes in Figure 4 represent the sensitivity of each sensor to the given vapor. Figure 4a shows the results of octane tested on MPC-coated QCM sensors. As seen in this figure, nanoparticles with low polarity surface ligands, such as AuC8, show slightly higher mass absorption sensitivity, based on the larger slope of its calibration line. When the same set of QCM sensors was tested with butyl acetate, AuEster showed the highest sensitivity in absorption mass increase. Both mixed ligand MPCs showed only marginal performance in QCM.

Figure 4. Calibration curves of octane and butyl acetate tested on QCM and chemiresistor array coated with four different MPCs. (♦:AuC8, ■:AuEster, ▲:MixCOOH, ×:MixPT).
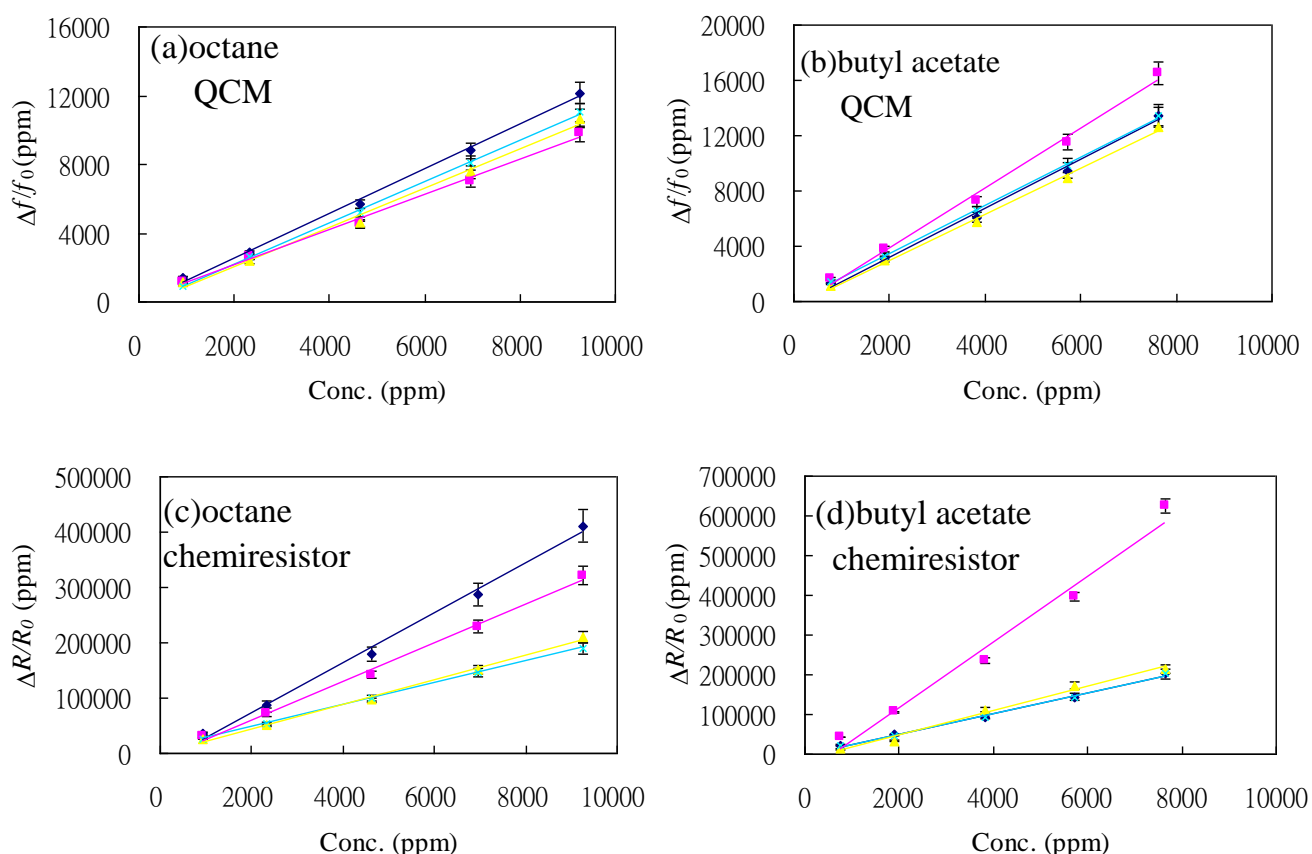
Although the test gas concentrations were high, we did not observe any "condensed liquid" on surface. In addition, the calibration lines (Figure 4) were linear all the way through the origin which indicated the response at lower concentration should fall in the prediction of calibration lines. The reason that we cannot perform tests with lower concentration is the sensitivity limit of the QCM sensor. As can be seen in Figure 3, the resolution limit of the QCM signal is 1 Hz in our system. The response of a few ppm concentrations is smaller than our detection limit. Both the swelling and dielectric changes of the film occurred simultaneously upon the vapor sorption. It is noted that an

increase in the swelling results in an increase of the film resistance while an increase in dielectric constant reduces the film resistance. As we have presented in our discussion session of the paper, these two factors cannot be differentiated in our tests. However, the contribution of the dielectric effect should be minor based on two reasons: first, all responses show a significant increase in the film resistance. Second, the chemical structure of the thiol monolayer is similar to those of tested vapors (*i.e.*, alkanes, esters, *etc.*).

The same set of MPCs was coated on IDE to form chemiresistors. The calibration curves of these chemiresistors are shown in Figure 4c,d. The sensitivity order *versus* that of octane is AuC8 > AuEster > MixCOOH ≈ MixPt. This order clearly differs from that of the QCM sensors with the same material. Dramatic changes in sensitivity were also observed when butyl acetate was tested. AuEster shows a substantially higher sensitivity than the other three MPC chemiresistors. By comparing Figure 4a with Figure 4c and comparing Figure 4b with Figure 4d, it is clear that the same set of sensing material shows diversified selectivity on different platforms. This is mainly because these two sensor platforms probe different MPC properties during vapor absorption. The frequency shift of the QCM is proportional to the absorbed masses of vapor molecules while the resistance change of the chemiresistor is the result of the combination of the swelling and dielectric effects.

3.3. Response Patterns of the MPC-Coated Sensor Array

When the responses of the same sensor platform (*i.e.*, QCM or IDE) are combined with different coating materials, it can be treated as a monotype sensor array. The response patterns can be derived by normalizing the sensitivities of all sensors with respect to the sensor with the highest sensitivity. The response pattern is a useful visualization tool to determine whether a combination of sensing materials provides the desired selectivity and, ideally, shows distinguishable patterns for various compounds. Figure 5 shows the response patterns of six VOCs tested on the QCM array of four MPCs. As Figure 5 shows, the patterns of these compounds differed only marginally, because QCM directly responds to the absorbed mass on surfaces. This result indicates that the MPCs are all equally sorptive, exhibiting a minor differentiation of the functional groups that exist in the interior of the surface monolayer.

When the same set of four MPCs was coated on IDEs to produce a chemiresistor array, the response patterns differed dramatically from the patterns generated by the QCM sensors. This is remarkable because they are essentially the same sensing material. For example, the resistive sensitivity of non-polar octane shows the highest sensitivity on AuC8, as in the QCM sensor; however, the ratios are different. The low polarity toluene showed almost the same sensitivity to both AuC8 and MixCOOH. The AuEster-coated chemiresistor showed outstanding performance when sensing polar VOCs.

The reason for the differences between Figures 5 and 6 lies in the sensing mechanisms that measured different properties of the same MPCs. The QCM revealed the mass increase during absorption, which is proportional to the partition coefficients of the given vapor and MPCs. The chemiresistor measured the swelling induced by absorption and the minor contribution of dielectric constant changes. Both sensors responded linearly to the increase in absorbed quantity, as shown in the excellent linearity of the calibration curve. However, the degree of swelling differed substantially among these MPCs. When vapor molecules are absorbed into an MPC film, the swelling can be

accounted for by the added free volume associated with the amount of adsorbates. This is fundamentally true for non-polar systems such as an AuC8 chemiresistor responding to octane. This behavior was accurately modeled by Stiencker *et al.* [18]. When the polarities of VOCs and MPCs increase, the attraction between them increases. This can result in the increase in partition coefficients and thus the responses on the QCM. However, the strong attraction causes the vapor molecules to tightly attach to the functional group on MPCs and reduce the effective free volume for swelling.

Figure 5. Response patterns of six VOCs measured by QCMs coated with four different MPCs.
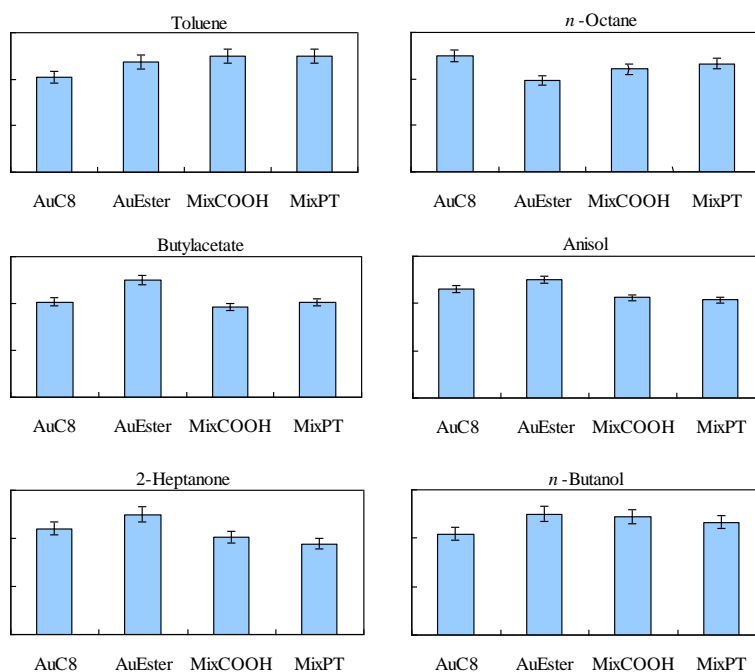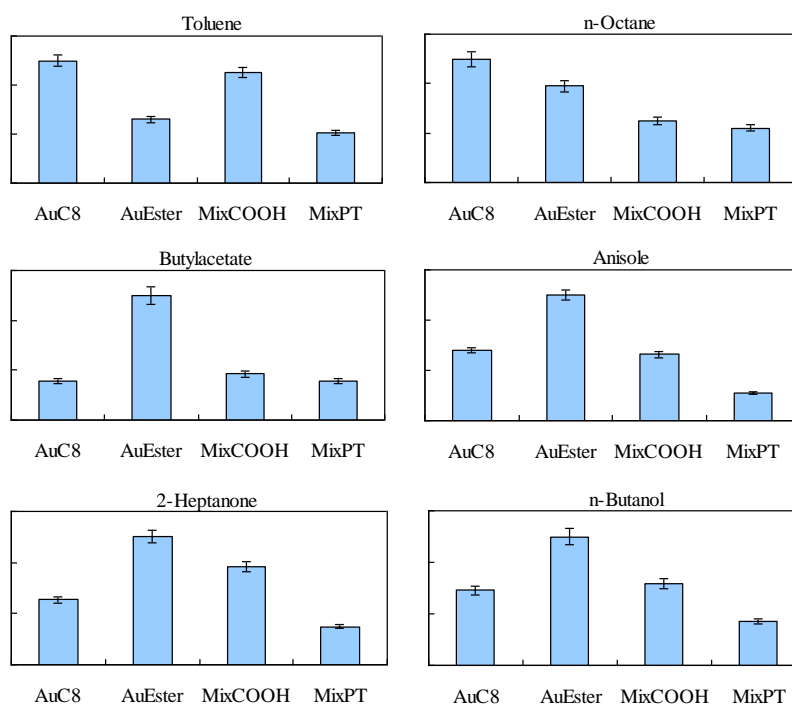

Figure 6. Response patterns of six VOCs measured by chemiresistors coated with four different MPCs.

Another factor that causes the difference in response patterns between QCMs and the chemiresistors is the interparticle attractions. The interparticle attractions arise because of surface polar groups. For instance, a dipole-dipole attraction can be produced between two aprotic polar groups, a π-electron stacking exists between the conjugating ring systems such as naphthalene thiol, or a hydrogen bond can be existed between acid-base paired surface functional groups. These forces can result in difficulties in swelling, hence the low sensitivity of chemiresistors. This factor did not negatively influence the response of the QCM because only the change of the mass was detected by the QCM. Our previous study used short chained and highly polar thiolates such as 2-benzothiazolethiol and 4-methoxythiolphenol to modify the Au nanoparticle surface [20]. The results in that study showed clearly distinguishable patterns on the QCM array but not on the chemiresistor array [21,22]. Most of the VOC response patterns look highly similar because of the outstanding sensitivity of AuC8 to the chemiresistor sensor. The short and polar functional groups tightly held MPCs together. When the absorbed vapor molecules could not diffuse into the region where nanoparticles were in contact with surrounding nanoparticles, the swelling became less efficient. In the current study, we used isooctyl 3-mercapropionate, which has a long and nonpolar group on the outside and a polar group on the inside. With this structure, we successfully created polar-compound sensitive MPCs that can outperform AuC8 when detecting many polar VOCs.

We also tested the possibility of using mixed thiolates with a long nonpolar chain and a short polar chain. The long alkane chain was used as a divider to reduce surface attraction. The process was replacing part of the surface ligand of the already synthesized AuC8 with small polar thiolates. The test results show that the combination of octanethiol and 3-mercaptopropionic acid on Au nanoparticles (MixCOOH) provides an improved performance on heptanone and similar sensitivity on anisole, compared with the original AuC8. This result proved that the sensor selectivity can be altered by using partial COOH group replacement. However, another example, MixPT, was unsuccessful. The responses of MixPT are always the least sensitive in chemiresistor arrays. It is possible that excessive 4-pyridinethiol replaces octanethiol on the surface, causing interparticle attraction to increase.

4. Conclusions

In this study, we synthesized and tested four MPCs on both QCM and chemiresistor sensors. The vapor sorption responses are rapid and reversible, which indicates that the nanoparticle film is highly permeable for VOCs. Although both the QCM and the chemiresistor responded linearly to VOC concentrations, the relative sensitivities (*i.e.*, selectivities) are not the same. The quantity of vapor absorption can be directly observed on the QCM frequency shift. However, the minor changes in surface polarity and interparticle attraction can only be reflected by chemiresistor selectivity. To obtain highly sensitive MPC material for chemiresistor sensors, reducing surface attraction is essential for maintaining effective swelling. The materials examined in this study can provide the preliminaries for the design of highly sensitive and selective monolayer-protected Au nanoclusters for resistor-type sensor applications.

Acknowledgments

Conflicts of Interest

The authors declare no conflicts of interest.

References

1. Mizukoshi, A.; Kumagai, K.; Yamamoto, N.; Noguchi, M.; Yoshiuchi, K.; Kumano, H.; Yanagisawa, Y. A novel methodology to evaluate health impacts caused by VOC exposures using real-time VOC and holter monitors. *Int. J. Environ. Res. Public Health* **2010**, *7*, 4127–4138.

2. Lin, Z.D.; Young, S.J.; Hsiao, C.H.; Chang, S.J. Adsorption sensitivity of Ag-decorated carbon nanotubes toward gas-phase compounds. *Sens. Actuator B Chem.* **2013**, *188*, 1230–1234.

3. Taurino, A.M.; Capone, S.; Siciliano, P.; Toccoli, T.; Boschetti, A.; Guerini, L.; Iannotta, S. Nanostructured TiO_2 thin films prepared by supersonic beams and their application in a sensor array for the discrimination of VOC. *Sens. Actuator B Chem.* **2003**, *92*, 292–302.

4. Chen, K.J.; Lu, C.-J. A vapor sensor array using multiple localized surface plasmon resonance bands in a single UV–vis spectrum. *Talanta* **2010**, *81*, 1670–1675.

5. Brust, M.; Bethell, D.; Schiffrin, D.; Kiely, C. Novel gold-dithiol nano-networks with non-metallic electronic properties. *Adv. Mater.* **1995**, *7*, 795–797.

6. Zamborini, F.P.; Leopold, M.C.; Hicks, J.R.; Kulesza, P.J.; Malik, M.A.; Murray, R.W. Electron hopping conductivity and vapor sensing properties of flexible network polymer films of metal nanoparticles. *J. Am. Chem. Soc.* **2002**, *124*, 8958–8964.

7. Wohltjen, H.; Snow, A.W. Colloidal metal−insulator−metal ensemble chemiresistor sensor. *Anal. Chem.* **1998**, *70*, 2856–2859.

8. Konvalina, G.; Haick, H. Sensors for breath testing from nanomaterials to comprehensive disease detection. *Acc. Chem. Res.* **2013**, doi:10.1021/ar400070m.

9. Hakim, M.; Broza, Y.Y.; Barash, O.; Peled, N.; Phillips, M.; Amann, A.; Haick, H. Volatile organic compounds of lung cancer and possible biochemical pathways. *Chem. Rev.* **2012**, *112*, 5949–5966.

10. Dovgolevsky, E.; Konvalina, G.; Tisch, U.; Haick, H. Monolayer-capped cubic platinum nanoparticles for sensing nonpolar analytes in highly humid atmospheres. *J. Phys. Chem. C* **2010**, *114*, 14042–14049

11. Evan, S.D.; Johnson, S.R.; Cheng, Y.L.; Shen, T. Vapour sensing using hybrid organic–inorganic nanostructured materials. *J. Mater. Chem.* **2000**, *10*, 183–188.

12. Segev-Bar, M.; Shuster, G.; Haick, H. Effect of perforation on the sensing properties of monolayer-capped metallic nanoparticle films. *J. Phys. Chem. C* **2012**, *116*, 15361−15368.

13. Rowe, M.P.; Plass, K.E.; Kim, K.; Kurdak, C.; Zellers, E.T.; Matzger, A.J. Single-phase synthesis of functionalized gold nanoparticles. *Chem. Mater.* **2004**, *16*, 3513–3517.

14. Kim, S.K.; Chang, H.; Zellers, E.T. Microfabricated gas chromatograph for the selective determination of trichloroethylene vapor at sub-parts-per-billion concentrations in complex mixtures. *Anal. Chem.* **2011**, *83*, 7198–7206.

15. Han, L.; Daniel, D.R.; Maye, M.M.; Zhong, C.-J. Core−shell nanostructured nanoparticle films as chemically sensitive interfaces. *Anal. Chem.* **2001**, *73*, 4441–4449.

16. Pang, P.F.; Guo, Z.D.; Cai, Q.Y. Humidity effect on the monolayer-protected gold nanoparticles coated chemiresistor sensor for VOCs analysis. *Talanta* **2005**, *65*, 1343–1348.

17. Konvalina, G.; Haick, H. Effect of Humidity on nanoparticle-based chemiresistors: A comparison between synthetic and real-world samples. *ACS Appl. Mater. Interfaces* **2012**, *4*, 317−325.

18. Steinecker, W.H.; Rowe, M.P.; Zellers, E.T. Model of vapor-induced resistivity changes in gold−thiolate monolayer-protected nanoparticle sensor films. *Anal. Chem.* **2007**, *79*, 4977–4986.

19. García-Berríos, E.; Gao, T.; Theriot, J.C.; Woodka, M.D.; Brunschwig, B.S.; Lewis, N.S. Response and discrimination performance of arrays of organothiol-capped Au nanoparticle chemiresistive vapor sensors. *J. Phys. Chem. C* **2011**, *115*, 6208–6217.

20. Yang, C.-Y.; Li, C.-L. Lu, C.-J. A vapor selectivity study of microsensor arrays employing various functionalized ligand protected gold nanoclusters. *Anal. Chim. Acta* **2006**, *565*, 17–26.

21. Li, C.-L.; Lu, C.-J. Establishing linear solvation energy relationships between VOCs and monolayer-protected gold nanoclusters using quartz crystal microbalance. *Talanta* **2009**, *79*, 851–855.

22. Li, C.-L.; Chen, Y.-F.; Liu, M.H.; Lu, C.-J. Utilizing diversified properties of monolayer protected gold nano-clusters to construct a hybrid sensor array for organic vapor detection. *Sens. Actuator B Chem.* **2012**, *169*, 349–359.